minerals

MDPI

Article

Microwave Treatment of Ultramafic Nickel Ores: Heating Behavior, Mineralogy, and Comminution Effects

Erin R. Bobicki [1,*], Qingxia Liu [2] and Zhenghe Xu [2]

[1] Department of Materials Science and Engineering, University of Toronto, Toronto, ON M5S 3E4, Canada
[2] Department of Chemical and Materials Engineering, University of Alberta, Edmonton, AB T6G 1H9, Canada; Qingxia2@ualberta.ca (Q.L.); zhenghe.xu@ualberta.ca (Z.X.)
* Correspondence: erin.bobicki@utoronto.ca

Received: 28 September 2018; Accepted: 4 November 2018; Published: 11 November 2018

Abstract: Ultramafic nickel ores are difficult to process because they contain serpentine, an anisotropic mineral with a nonspherical morphology and multiple pH-dependent surface charges. Dehydroxylation of serpentine in ultramafic nickel ores by microwave treatment is proposed to improve the processability of these ores. Upon heating, serpentine is converted to olivine, an isotropic mineral that is benign in mineral processing circuits. The microwave heating of two ultramafic nickel ores is explored in this paper, as well as effects on mineralogy and grindability. The first ore was sourced from the Okanogan nickel deposit in Washington State, USA, while the second ore was obtained from the Vale-owned Pipe deposit located in the Thomson Nickel Belt in Manitoba, Canada. The ultramafic nickel ores were found to heat well upon exposure to microwave radiation and the heating behaviors were a function of the imaginary permittivities. The temperatures achieved during microwave treatment were sufficient to dehydroxylate serpentine, and the serpentine content in ultramafic nickel ores was reduced by 63–84%. The grindability of ore with consistent texture (OK ore) improved dramatically with microwave treatment, whereas the grindability of ore with inconsistent texture (Pipe ore) was found to decrease. Pentlandite liberation and specific surface area improved for both ores with microwave treatment. Ultimately, microwave pretreatment did not decrease the energy required for grinding under the conditions studied. However, energy savings may be realized when overall process improvements are considered (e.g., grinding, rheology, flotation, material handling, dewatering and tailings treatment).

Keywords: mineral processing; microwave; permittivity; ultramafic ores; comminution; mineralogy

1. Introduction

Ultramafic nickel ores are difficult to process, and the difficulty is largely due to the presence of serpentine ($Mg_3Si_2O_5(OH)_4$). Serpentine is an anisotropic mineral with multiple pH-dependent surface charges and a nonspherical morphology. The processing of ultramafic nickel ores involves upgrading by froth flotation, on which serpentine minerals have a particularly negative effect. The surface charge of the serpentine brucite-like basal plane is opposite that of the valuable nickel-bearing mineral, pentlandite ($(Ni,Fe)_9S_8$), at the pH of flotation (pH 9–10) [1]. Hence, serpentine slime-coats pentlandite during flotation and renders it unrecoverable [2]. Fibrous serpentine (chrysotile) can form fiber-bubble aggregates that report to the froth, resulting in a diluted concentrate and creating problems downstream in smelting operations [3]. Serpentine also greatly increases the viscosity of ore slurries due to its morphology and anisotropic nature [1,4,5], which inhibits the separation of minerals and necessitates that grinding and flotation be conducted at low solids content [3,6]. Thus, it is hypothesized that the

destruction of serpentine minerals in ultramafic nickel ores by dehydroxylation should be beneficial for mineral processing. The dehydroxylation of serpentine results in the formation of olivine (Mg_2SiO_4) (Reaction (1)).

$$2Mg_3Si_2O_5(OH)_4 \xrightarrow{heat} 3Mg_2SiO_4 + SiO_2 + 4H_2O \quad \text{(Reaction 1)}$$

Olivine is not fibrous or anisotropic, has an isoelectric point close to that of pentlandite, and the interaction between olivine and pentlandite is strongly repulsive [2]. Thus, the negative effects of serpentine on grinding and flotation, including slime coating, froth dilution by fiber-bubble aggregates, and high viscosity, should be reduced or eliminated by serpentine dehydroxylation.

The dehydroxylation of serpentine in ultramafic nickel ores by microwave treatment as part of mineral processing operations is proposed. The treatment would be conducted prior to grinding, to ensure the ore would be relatively dry (most grinding in mineral processing is conducted in the aqueous phase), thus limiting energy wastage due to the evaporation of water, and after crushing, to ensure the particle size would be not only more uniform but appropriate for penetration by microwaves. Conducting the treatment prior to grinding would also allow any benefits of microwave-induced fracture to be exploited. The flotation tailings produced from microwave pretreated ultramafic nickel ores could also be suitable for mineral carbon storage [7]. A schematic of the proposed flowsheet is depicted in Figure 1.

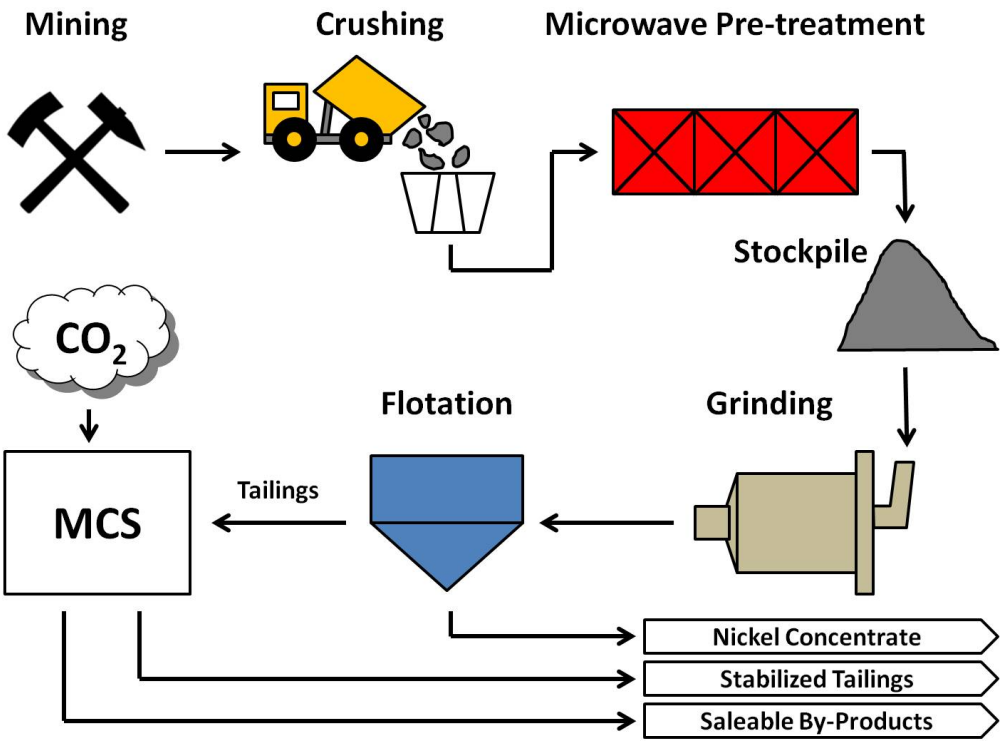

Figure 1. Schematic of a combined mineral processing and mineral carbon storage (MCS) process with microwave pretreatment.

Microwaves are electromagnetic radiation with frequencies of 0.3–300 GHz and wavelengths of 0.001–1 m. The internationally recognized frequency bands used for industrial and domestic applications are 915 and 2450 MHz [8], respectively, and electrical energy is converted to microwave energy with efficiencies of 85% and 50% for these frequencies [9]. Advantages of microwave heating include that it is efficient, noncontact, rapid, and material selective [9]. Microwaves have been applied in a number of different metallurgical applications including drying, grinding, leaching, calcination, sintering, reduction, roasting/smelting, and spent carbon regeneration, and have been used for

the processing of oxide ores, slags, electric arc furnace dust, gaseous effluents and gold-bearing materials [9,10].

Microwave applications in mineral processing have primarily been focused on microwave-assisted comminution in an effort to improve the energy efficiency of this process, which can be very low (<1%) [11]. Conventional size reduction involves the application of mechanical energy to break a particle into finer units. The greater the number of imperfections in a particle, the more easily it will break under mechanical stress. Since minerals have varying microwave absorption characteristics, different minerals within the same particle heat differentially upon exposure to microwaves. The differential heating of constituent minerals generates thermal stresses within particles and can lead to fracture. The fracturing often occurs along mineral grain boundaries, which can result in improved mineral liberation and grinding efficiency [12,13]. A number of researchers have reported an improvement in the grindability of ores and the liberation of valuable minerals after microwave treatment [12–17].

In general, microwave-assisted comminution appears to be most effective for ores composed of minerals that are good absorbers of microwave radiation in a transparent gangue matrix [18]. Ultramafic nickel ores seem to fit this description, containing mostly serpentine, which is not a good absorber of microwave energy [19], and lesser concentrations of highly microwave responsive minerals, including magnetite, pentlandite and pyrrhotite [20]. The presence of highly microwave responsive minerals in ultramafic nickel ores should also allow the temperatures required for serpentine dehydroxylation (600–700 °C [21]) to be achieved during microwave treatment. The objective of this paper is to explore the microwave heating of ultramafic nickel ores and effects on the mineralogy, ore grindability, specific surface area and pentlandite liberation. The results are discussed with respect to mineral processing and energy usage in comminution.

2. Materials and Methods

2.1. Feedstock

Two low-grade ultramafic nickel ores were used in this study. The first, referred to as the "OK ore", was obtained from the Okanogan nickel deposit in Washington State, USA. The second ore, referred to as the "Pipe ore", was sourced from the Vale-owned Pipe deposit located in the Thomson Nickel Belt, in Manitoba, Canada. The OK ore was received as cobbles of 9–20 cm. It was crushed to <2.5 mm using a jaw crusher (BB 200, Retsch, Burlington, ON, Canada). The Pipe ore was received pre-crushed to <2 mm. Further dry size reduction of the ores was achieved using a disc mill (DM 200, Retsch, Burlington, ON, Canada). Both ores were sieved to isolate the 0.425–1 mm and 1–2 mm size fractions, and split into 100 g samples for microwave treatment using a Jones riffle sample splitter. Elemental composition of the OK and Pipe ores is shown in Table 1.

Table 1. Elemental composition of OK and Pipe ores.

	MgO	**CaO**	**SiO_2**	**Al_2O_3**	**Fe**	**Ni**	**S**
Method	XRF	XRF	XRF	XRF	ICP	ICP	CHNS
OK Ore (wt %)	45.8	0.8	40.7	1.1	4.6	0.26	0.66
Pipe Ore (wt %)	39.5	1.1	34.8	1.8	6.0	0.23	2.18

The OK ore consisted of mostly of serpentine (84.0 wt %), with lesser amounts of magnetite (6.6 wt %, Fe_3O_4), brucite (5.1 wt %, $Mg(OH)_2$) and pentlandite (4.3 wt %). The Pipe ore was also primarily composed of serpentine (63.7 wt %), as well as magnetite (12.3 wt %), olivine (7.7 wt %), dolomite (5.5 wt %, $CaMg(CO_3)_2$), pyrrhotite (4.7 wt %, $Fe_{1-x}S$), pentlandite (2.8 wt %), and trace quartz, cordierite and vermiculite.

2.2. Microwave Heating

A 1000 W, 2.45 GHz household microwave oven manufactured by Panasonic (NN-SF550M Flat and Wide) was used for microwave treatment at 100% power. The microwave oven was modified to permit purge gas to flow through a reactor stationed inside the oven. Microwave leakage was tested after modification of the microwave oven and found to be well below legal limits. The microwave reactor was fabricated of quartz and insulated with ceramic wool. 100 g samples of crushed ore were placed in a 100 mL quartz crucible, which was then placed in the microwave reactor. During microwave treatment, the reactor was purged continuously with 1 L/min of nitrogen gas to limit oxidation of the sample. To establish microwave-heating curves, ore samples were exposed to microwave radiation for different increments of time. Immediately following treatment, the samples were removed from the reactor and the temperature of the samples was determined by inserting the tip of a Type K thermocouple into the center of the sample. In all other tests, samples were cooled for two hours in the microwave reactor under a nitrogen atmosphere to prevent oxidation.

2.3. Grinding

One-hundred-gram samples of 0.425–1 mm ore were ground aqueously at 30 wt % solids in a stirred attrition mill (01-HD Laboratory Attritor, Union Process, Akron, OH, USA) with alumina media (Union Process). The standard grinding time was 15 min. The relative work index (RWI) method described by Berry and Bruce [22], as given by Equation 1, was used to assess the effect of microwave pretreatment on the grindability of the ores, where P and F are the 80% passing size in μm of the product and feed materials respectively, r refers to the reference sample (untreated) and t refers to the test sample (microwave pretreated). A RWI of 100% indicates no change in grindability, while a RWI of less than 100% indicates improved grindability and smaller product size, and a RWI greater than 100% indicates poorer grindability and a larger product size.

$$RWI = \left[\left(\frac{10}{\sqrt{P_r}} - \frac{10}{\sqrt{F_r}}\right) \Big/ \left(\frac{10}{\sqrt{P_t}} - \frac{10}{\sqrt{F_t}}\right)\right] \times 100\% \quad (1)$$

2.4. Materials Characterization

X-ray fluorescence (XRF) spectroscopy (Orbis PC Micro-EDXRF Elemental Analyzer, EDAX, Mahwah, NJ, USA) was used to determine the elemental composition of the ores for elements heavier than sodium. Powdered samples were pressed into 1-inch diameter pellets for analysis. The XRF microprobe was operated at 40 kV and 250 μA and the X-ray source was monochromatic Rh Kα radiation. Inductively coupled plasma mass spectrometry (ICP-MS) (Perkin Elmer Elan 6000, Waltham, MA, USA) was also used to determine the elemental composition of the ores. A mixture of 0.2 g of powered sample, 5 mL HNO_3 and 5 mL HF was heated on a hot plate for 48 h. The sample was then dried and mixed with 5 mL HNO_3 and 5 mL HCl and heated for a further 24 h on a hot plate. After the second heating, the sample was dried again, then combined with 8 N HNO_3 and analyzed. Sulphur analysis was conducted using a combustion technique (Vario MICRO Cube, Elementar, Hanau, Germany). Quantitative XRD analysis was performed on several samples using the Rietveld refinement technique by PMET Inc. of New Brighton, Pennsylvania, USA. The mineral composition of the ores was also assessed in-house by qualitative X-ray diffraction (XRD) (Rigaku XRD System, Rigaku, ON, Canada). Fourier transform infrared spectroscopy (FTIR) was used to identify changes in the molecular structure of ore samples. Infrared spectra were collected across the mid-infrared range (4000–400 cm^{-1}) using a Bio-Rad FTS 6000 Fourier Transform Infrared Spectrophotometer (Bio-Rad Laboratories, Hercules, CA, USA). Samples were diluted in powdered potassium bromide (KBr) at concentration of 5% for analysis. The collected spectra were interpreted by comparison to spectra reported in the literature.

The relative real and imaginary permittivities of the Pipe and OK ores were determined using the Cavity Perturbation Measurement Technique [23] by Microwave Properties North (Deep River,

Ontario). Measurements were conducted at two frequencies, 912 and 2466 MHz, in an argon gas atmosphere. Measurements were taken at room temperature, 50 °C, and then in 50 °C increments up to 1150 °C.

The particle size distribution of samples was determined using sieving techniques (Fisherbrand Sieves, Tyler Rotap) for particles >250 µm, and a light scattering technique (Mastersizer 2000, Malvern Instruments Ltd., Malvern, Worchestershire, UK) for particles <250 µm. Light scattering, along with the use of sonication and a dispersant, were required to assess the particle size distribution of <250 µm particles due to the severe aggregation of particles in this size class.

Microhardness measurements (Tukon 1102 Knoop/Vickers Hardness Tester, Buehler, Lake Bluff, IL, USA) were performed on 1–2 mm ore particles set in resin and polished using the Vickers microhardness testing standard outlined in ASTM E384-11 (ASTM, 2012). Mineral liberation analysis (MLA, FEI Company, Brisbane, Australia) was conducted on ore samples after grinding by Vale Base Metals Technology Development (Mississauga, ON, Canada). The surface area of samples after grinding was determined by the multipoint Brunauer–Emmett–Teller (BET) method using an automated Autosorb-1 gas sorption analyzer (Quantachrome Instruments, Boynton Beach, FL, USA).

Scanning electron microscopy (SEM) was used to study pretreated and untreated ore. Prior to the analysis, ore samples were set in resin, polished to reveal particle cross-sections, and coated with carbon (to minimize charging effects). A Hitachi S-2700 Scanning Electron Microscope equipped with a Princeton Gamma-Tech IMIX digital imaging system was used to obtain the micrographs. A PGT PRISM Intrinsic Germanium detector was used for EDX (energy dispersive X-ray) analysis and BSE (backscattered electron) analysis was performed using a GW Electronics 47 four quadrant solid-state backscattered electron detector. The probe was operated with an accelerating voltage of 20 kV and a current of 0.5 nA. The working distance was 17 mm. The degree of cracking present in ore samples was determined by measuring the crack length per unit area (Image Pro Plus 7.0 software, Media Cybernetics, Rockville, MD, USA) visible in SEM images of polished cross-sections of randomly selected 0.425–1 mm unground particles.

3. Results and Discussion

3.1. Microwave Heating

The temperature and mass loss of the OK and Pipe ores versus microwave heating time is shown in Figure 2. The heating rates are shown in Figure 3. Both ores heated well in response to microwave treatment, and heated significantly better than pure serpentine, the primary component of both ores (Forster et al. [19] reported that 7.5 g of serpentine reached a maximum temperature of 216°C after 20 min of heating time in a 1.2 kW 2450 MHz microwave oven). Despite similarities in mass loss with microwave heating time, the OK and Pipe ores demonstrated disparate heating behavior, which particularly diverged at longer microwave exposure times. The OK ore had a high initial heating rate that declined with increasing temperature and microwave exposure time. The OK ore reached a maximum bulk temperature of 730 °C after 15 min heating time, corresponding to a mass loss of 11.8%. The Pipe ore also demonstrated a high initial heating rate that declined with increasing temperature and microwave exposure time up until 8 min microwave heating time. After 8 min of microwave exposure, however, an increase in heating rate was observed, at which point the sample partially melted. The melted portion of the sample fused upon cooling; hence, a maximum microwave treatment time of 8 min was used for all further test work with the Pipe ore. Overall, this treatment resulted in samples that were most comparable to OK ore samples microwave treated for 15 min. The Pipe ore attained a maximum bulk temperature of 1073 °C after 15 min microwave heating time, which corresponded to a mass loss of 12.4%.

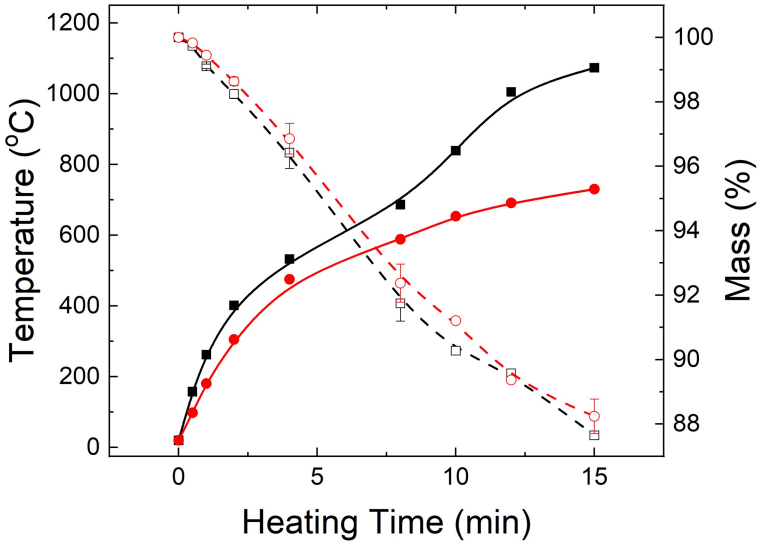

Figure 2. Temperature (solid markers) and mass loss (open markers) as a function of microwave heating time for Pipe (■, □) and OK (●, ○) ores.

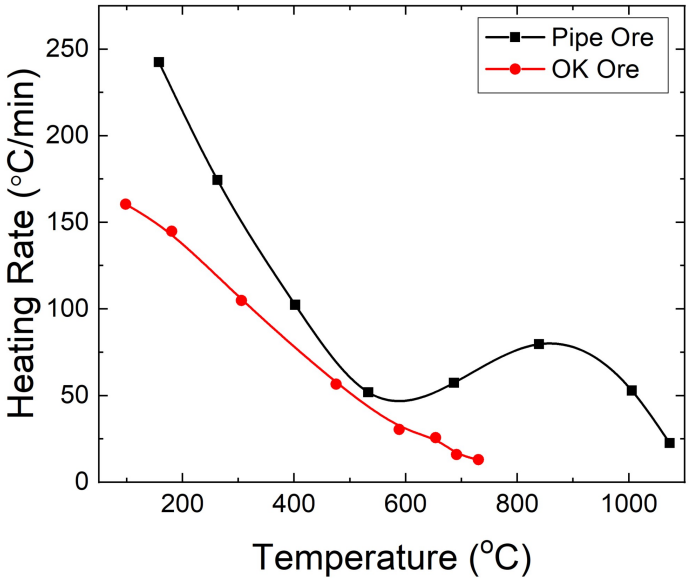

Figure 3. Heating rate upon exposure to microwave radiation versus temperature for Pipe and OK ores.

The heating behavior of a material upon exposure to microwaves can be understood by examining the fundamental physics of microwave heating, and relating the observed heating behavior to intrinsic material properties. The heating rate of a material upon exposure to microwave radiation (Equation (2)) is directly proportional to the power dissipation (P(z)), and inversely proportional to the material density (ρ) and specific heat capacity (C_p).

$$\frac{dT}{dt} = \left(\frac{P(z)}{\rho C_p}\right) \tag{2}$$

Since the initial densities of the OK and Pipe ores were similar, and since the mass loss curves were nearly identical, density is not believed to have been responsible for the differences in the heating rate curves of the two ores. Similarly, the heat capacities of the two ores as a function of temperature, based on the composition of the ores and heat capacities reported in the literature for the constituent minerals [24], were also very similar. Thus, the difference in the heating rates of the two ores occurred

as a result of differences in power dissipation. The power dissipation (P(z)) of a dielectric material, defined as the ability of a material to absorb microwave power, is a function of microwave frequency (f), the relative imaginary permittivity (ε_r''), the permittivity of free space (ε_o), and the electric field intensity (E) (Equation (3)) [8].

$$P(z) = 2\pi f \varepsilon_o \varepsilon_r'' E^2 \quad (3)$$

The permittivity of free space is a constant, and the frequency and electric field intensity were also constant in the microwave heating tests. The imaginary permittivity of a material, however, can vary considerably with temperature. Imaginary permittivity is a measure of a material's ability to convert microwave energy into heat. A related parameter, measured concurrently with imaginary permittivity, is the real permittivity. Real permittivity reflects the ability of a material to be polarized by an electric field. While both permittivity components contribute to the electric field distribution in a material, only the imaginary permittivity affects the heating rate. The imaginary and real permittivities of the Pipe and OK ores with increasing temperature are shown in Figure 4. The imaginary permittivity of the Pipe ore is substantially higher than that for the OK ore below 400 °C and above 700 °C. These are the temperature ranges over which the Pipe ore heating rate (Figure 2) is much larger than that for the OK ore. Thus, differences in the microwave heating behavior of the two ores can be attributed to differences in the imaginary permittivity. The real permittivity of the Pipe ore is also higher than that for the OK ore over the same temperature range (below 400 °C and above 700 °C), suggesting the Pipe ore is also better polarized by the microwave field at these temperatures. The nature of the permittivity curves will be explored in more detail in a separate study.

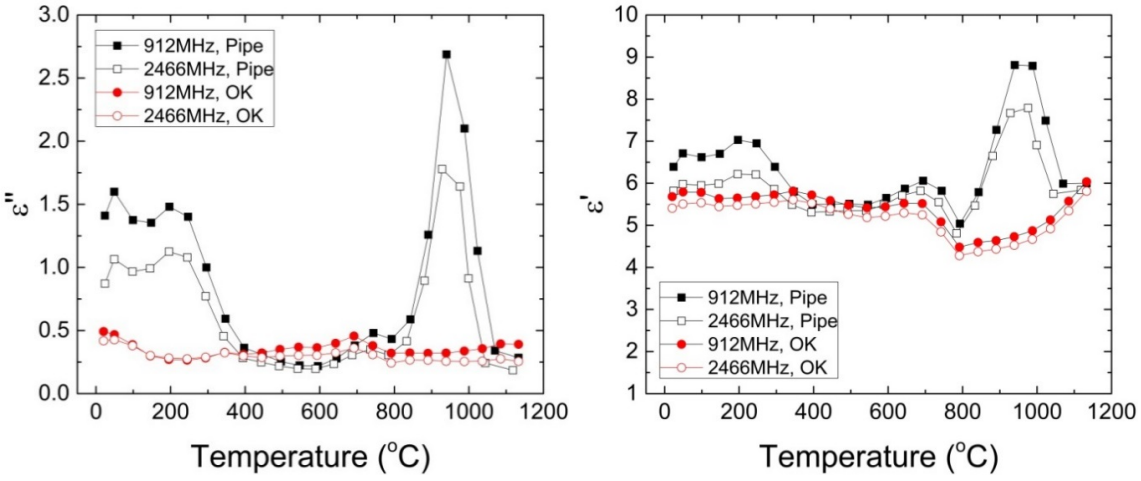

Figure 4. Imaginary permittivity (**left**) and real permittivity (**right**) for the Pipe and OK ores with increasing temperature at frequencies of 912 and 2466 MHz.

3.2. Mineralogy

3.2.1. XRD

The serpentine and olivine content in the Pipe and OK ores as determined by quantitative XRD is shown in Figure 5. Both ores were primarily composed of serpentine prior to microwave treatment. Microwave heating times up to 4 min had a negligible effect on the serpentine content; however, after 8 min microwave treatment time, serpentine began to breakdown and olivine was formed. A microwave treatment time of 15 min decreased the serpentine content in OK ore from 84.0 wt % to 15.8 wt % and increased the olivine content from 0 wt % to 80.2 wt %. A microwave treatment time of 8 min reduced the serpentine content in Pipe ore from 63.7 wt % to 23.7 wt % and increased the olivine content from 7.7 wt % to 51.1 wt %. The substantial conversion of serpentine to olivine in the Pipe and OK ores should be beneficial for mineral processing. A potentially negative impact of

microwave treatment of ultramafic nickel ores for mineral processing is that pentlandite was shown to be converted to another nickel phase that was not detected by XRD. Full quantitative XRD results for microwave pretreated Pipe and OK ores can be found in Bobicki et al. [25].

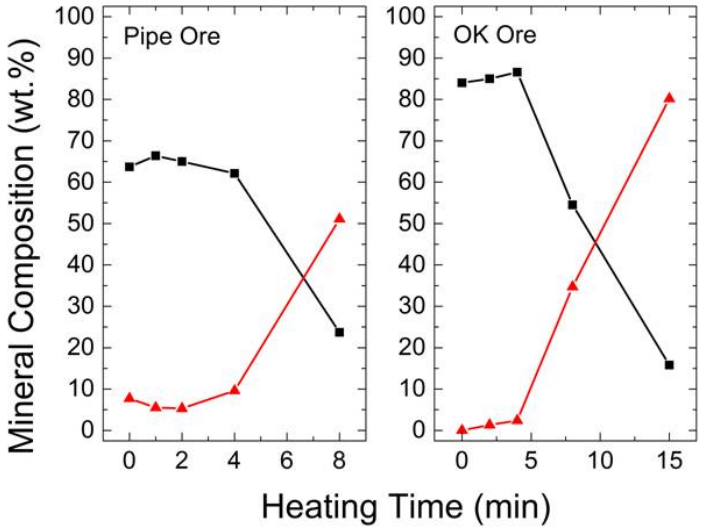

Figure 5. Serpentine (■) and olivine (▲) content of Pipe and OK ores as a function of microwave heating time.

3.2.2. FTIR

FTIR analysis was done to better understand the conversion of serpentine to olivine by microwave treatment. FTIR spectra collected for untreated and microwave pretreated Pipe and OK ore are shown in Figure 6. The spectra collected for all samples were similar, but with important differences. Three main adsorption bands were observed in the IR spectrum: the first in the 3700–3300 cm^{-1} region, the second in the 1100–800 cm^{-1}, and the third in the 800–500 cm^{-1} region. The peaks in the first region correspond to the stretching vibrations of the hydroxyl groups bonded to octahedrally coordinated cations in the serpentine brucite layer [26–30]. The main peak at 3687–3690 cm^{-1} in the Pipe and OK ore can be attributed to hydroxyl groups bonded to magnesium ions. The weaker peaks are the result of substitution by aluminum, nickel, and ferrous ions for magnesium (3668 cm^{-1}, 3650 cm^{-1} and 3575 cm^{-1}) [26,31,32]. The shoulder (tail towards lower wavenumbers) adjacent to the hydroxyl peaks indicates variations in M-OH bond strengths [28].

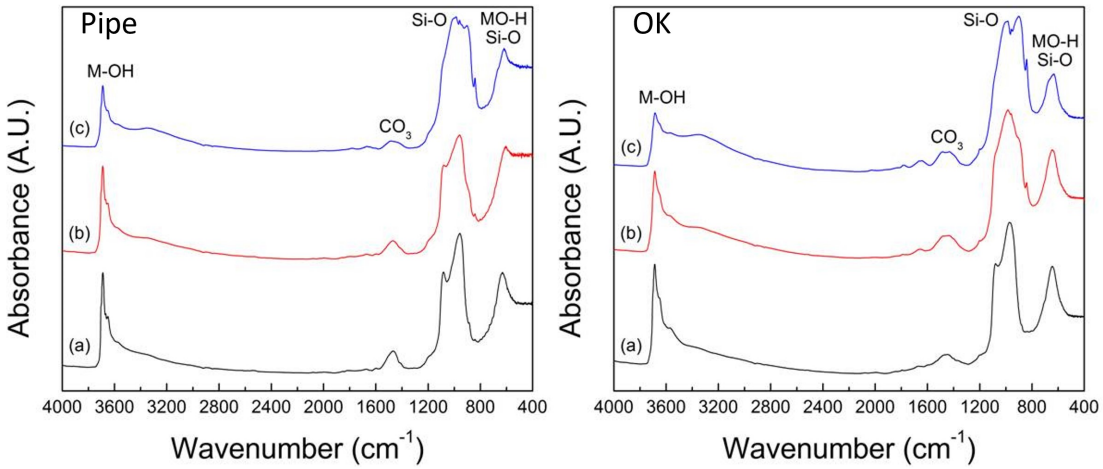

Figure 6. FTIR spectra obtained for Pipe ore (untreated (**a**) and microwave pretreated for 4 (**b**) and 8 (**c**) min) and OK ore (untreated (**a**) and microwave pretreated for 8 (**b**) and 15 (**c**) min).

The peaks in the second region are related to the vibrations of Si–O bonds. Some of the peaks are associated with the serpentine siloxane layer, including the 1074–1083 cm^{-1} bands (stretching of the apical Si–O bond perpendicular to the basal plane) and the 960–971 cm^{-1} bands (arising from the stretching of the basal Si–O–Si bonds that bridge pairs of corner-sharing Si tetrahedra) [26,28,29]. Other peaks, including those at 841–842 cm^{-1}, 886 cm^{-1}, 901–903 cm^{-1}, 957–960 cm^{-1} and 985 cm^{-1} are due to stretching vibrations of Si–O bonds in the isolated silica tetrahedra of olivine [33–35].

The origin of absorption in the 800–500 cm^{-1} range is more difficult to precisely define as many peaks overlap. In the case of serpentine, it appears absorption in this range may be attributed to the deformation of hydroxyl groups: bands in the range of 605–625 cm^{-1} can be attributed to the bending vibrations of MgO–H bonds on the inside of the brucite layer, whereas bands in the range of 640–650 cm^{-1} represent the vibrations of external MgO–H bonds [27,28,33]. In the case of olivine, bands near 600 cm^{-1} are reported to be the result of SiO_4 bending modes [35,36]. The minor peak at 1450 cm^{-1} can be attributed to the asymmetric stretching of carbonate groups [37,38].

Some differences between the OK and Pipe ore infrared spectra include the presence of olivine peaks in untreated Pipe ore and the position of weak hydroxyl peaks in region 1. The position of the weak hydroxyl peaks indicates that the substitution of Fe^{2+} for Mg^{2+} is dominant in the OK ore, whereas Al^{3+} and Ni^{2+} are substituted for Mg^{2+} more frequently in the Pipe ore. This correlates with the observation of Fe-substituted serpentine during SEM-EDX analysis.

Microwave pretreatment resulted in some interesting changes in the FTIR spectra. In both the OK and Pipe ore, the area under the hydroxyl peaks in Region 1 was diminished with increasing microwave treatment time, indicating that serpentine was progressively dehydroxylated. However, the area under the hydroxyl peaks did not diminish significantly until after 8 min microwave pretreatment for both the Pipe and OK ores, which agrees with the XRD data that showed the serpentine content of the ores did not decrease substantially until after 8 min of microwave treatment. In addition to the diminishment of the hydroxyl peaks in Region 1, the hydroxyl shoulder became more pronounced, indicating that remaining hydroxyl bonds were weakened. Also, an additional peak appeared in the OK and Pipe ores at 3352–3357 cm^{-1}. This peak can be attributed to Fe^{3+} substitution for Mg^{2+} in olivine [39]. In Region 2, the peaks shifted from peaks associated with serpentine to peaks associated with olivine. Furthermore, the olivine peak at 886 cm^{-1} in the Pipe ore disappeared, apparently overshadowed by the more intense olivine peak at 901 cm^{-1}. In Region 3, the area under the peaks in both OK and Pipe ores was diminished, and the peaks shifted to lower wavenumbers, indicating MgO–H bonds were broken and those that remained were weakened. It is also possible that the peaks remaining in this region after longer microwave treatment were actually the result of olivine SiO_4 bending modes. Interestingly, the serpentine Si–O peaks did not diminish in intensity until after the diminishment of the Mg–OH and MgO–H peaks. This indicates the octahedral brucite layer was disrupted during the microwave pretreatment of serpentine prior to the breaking apart of the tetrahedral siloxane layer. Trittschack and Groberty [40] observed a similar phenomenon during the conventional heat treatment of serpentine. Upon the collapse of the siloxane layer, olivine forms from the newly isolated silica tetrahedra surrounded by dehydroxylated octahedral magnesium, as evidenced by the subsequent increase in intensity of the Si–O peaks associated with olivine.

3.2.3. SEM

To better understand the effect of microwave treatment on the fate of nickel in the OK and Pipe ores, samples of untreated and pretreated OK and Pipe ore were analyzed by SEM-EDX. Figure 7a and 7c depict SEM-BSE images of untreated OK and Pipe ore respectively. Figure 7b shows an SEM-BSE image of OK ore microwave pretreated for 15 min and Figure 7d displays Pipe ore microwave pretreated for 8 min. The continuous dark grey material of various shades in the OK and Pipe ore SEM-BSE images was composed of magnesium, silicon, and oxygen. This material is the serpentine and olivine detected by XRD. The light grey material observed clearly in the SEM-BSE image shown of the untreated OK ore (Figure 7a) was similar in composition to the dark grey, although it also

contained iron. This material was most probably serpentine with iron substituted for magnesium in the octahedral layer. The bright white material in the SEM-BSE images of the OK and Pipe ore was composed of iron, nickel and sulphur in various ratios. Magnetite also appeared bright white in the SEM-BSE images, however, the texture was finer than the Fe-Ni-S material.

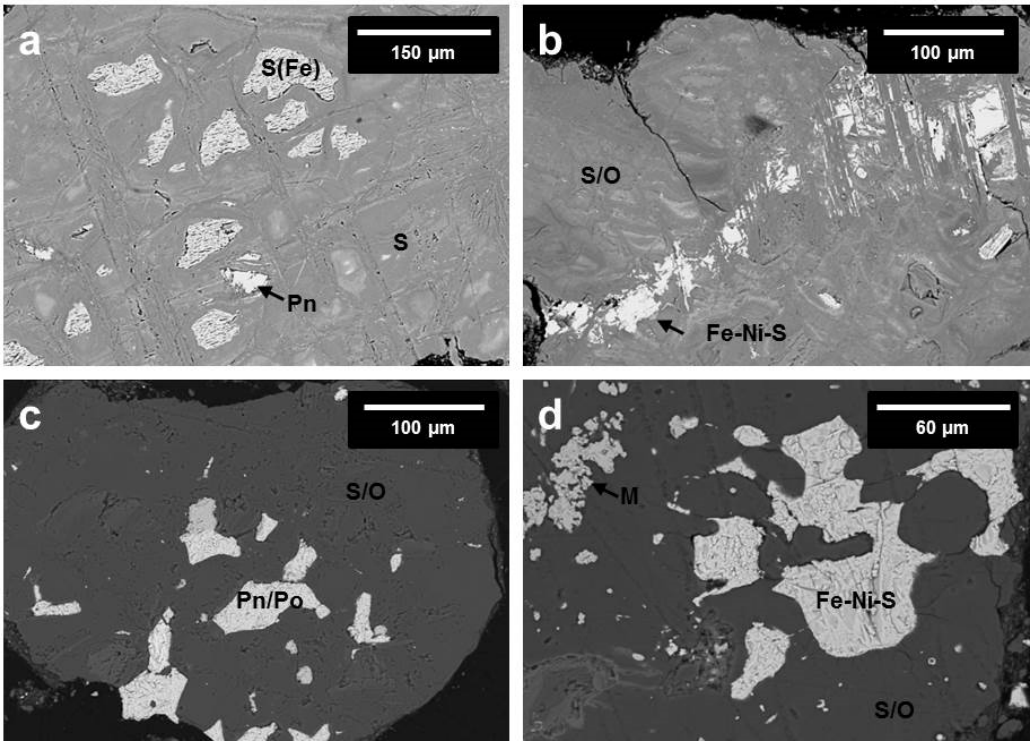

Figure 7. SEM-BSE images of (**a**) untreated OK ore, (**b**) OK ore microwave pretreated for 15 min, (**c**) untreated Pipe ore, and (**d**) Pipe ore microwave pretreated for 8 min. The phases are designated as follows: serpentine (S), iron-substituted serpentine (S(Fe)), olivine (F), pentlandite (Pn), pyrrhotite (Po), iron-nickel sulphide (Fe-Ni-S), and magnetite (M).

As is evident from the SEM-BSE images, nickel remained in a Fe-Ni-S phase in the Pipe and OK ores after microwave pretreatment. The Fe-Ni-S minerals observed in the microwave pretreated ores had metal-to-sulphur (M:S) ratios representative of pyrrhotite (high-sulphur) and pentlandite (low sulphur); however, the high-sulphur material was mostly nickel-rich (up to 23 at.%) while the nickel content of the low-sulphur material was variable, ranging from 1–36 at.%. Upon heating, pentlandite is reported to degrade to a monosulphide solid-solution (mss) of the formula $(Fe,Ni)_{1-x}S$ at temperatures above 610 °C [41,42]. Some researchers assert the mss coexists with a $Ni_{3\pm x}S$ phase [43,44], while others believe a high-temperature pentlandite solid solution (hpn) appears with mss at temperatures below 870 °C (above which hpn breaks down into mss and liquid) [45,46]. Upon quenching and cooling to room temperature, pentlandite re-forms from the high-temperature phases [41,43]. Under natural conditions (slow cooling, sulphur-rich composition, and presence of impurities), however, pentlandite is reported to exsolve over a period of 3,000 to 30,000 years [41]. Thus, it appears Ni remained in high-temperature phases after slow cooling in the microwave pretreated OK and Pipe ores. The transition of pentlandite to other nickel phases may have implications for mineral processing and the upgrading of ultramafic nickel ores by froth flotation.

3.3. Grindability

3.3.1. Product Size and Relative Work Index

The product size (P_{80}) and RWI resulting from the milling of microwave treated Pipe and OK ores are depicted in Figure 8. Microwave treatment of the OK ore drastically reduced the product size after milling and improved the grindability of the ore. The product size decreased with increasing pretreatment time from a P_{80} of 606 µm with no pretreatment to 19 µm after 15 min microwave pretreatment (RWI = 3.6%). Similar improvements in ore grindability as a result of microwave pretreatment have been observed by others [12,14,15,18]. In contrast, microwave treatment increased the product size of the Pipe ore and decreased the grindability. Without microwave pretreatment, the Pipe ore ground as well as the OK ore pretreated with microwaves for 15 min (P_{80} = 19 µm). With increasing microwave pretreatment time, the P_{80} and RWI of the Pipe ore increased with increasing microwave heating time up to a microwave exposure time of 4 min (P_{80} = 148 µm). After 8 min of microwave pretreatment, the P_{80} returned to a value near that of the untreated Pipe ore (P_{80} = 27 µm). Almost no instances of microwave pretreatment worsening the grindability of ore have been reported in the literature, with the exception of Kaya [47] who found the microwave pretreatment of a porphyry copper ore increased the bond work index by 7%. The researchers attributed the decrease in grindability to the fusion of chalcopyrite particles [47].

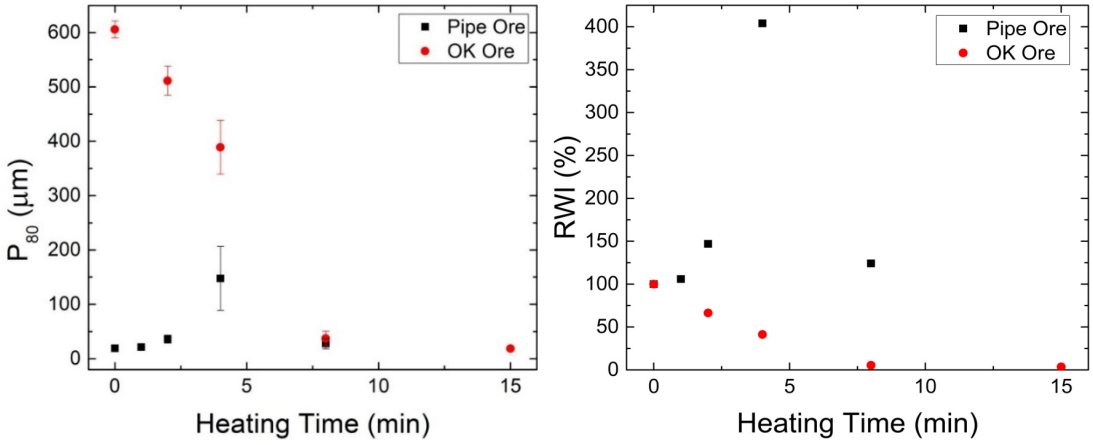

Figure 8. Product size (P_{80}) (**Left**) and RWI (**Right**) versus microwave heating time for Pipe and OK ores after grinding [48].

A breakdown of the particle size distributions into three broad size categories (>425 µm, 106–425 µm, and <106 µm) revealed that while particles in the OK ore were normally distributed regardless of microwave treatment time, particles in the Pipe ore were concentrated in the >425 µm and <106 µm size fractions (bimodal distribution). With increasing microwave treatment time up to 4 min, the percentage of particles in the large size fraction of the Pipe ore increased (mass of >425 µm fraction increased by 11%). The increase in large, unground particles in the Pipe ore suggests that some particles underwent a mineralogical change that made them harder and reduced their grindability. After 8 min microwave pretreatment, the percentage of particles in the large size fraction returned to a value similar to that for the untreated Pipe ore.

3.3.2. Size-By-Size Analysis

To determine if a harder mineral phase was formed in the Pipe ore during microwave treatment, and to compare the texture of the Pipe and OK ores, untreated and microwave treated Pipe and OK ore was sieved into three size fractions after grinding (>425 µm, 106–425 µm, and <106 µm) and analyzed by XRD. For the untreated OK ore, the three size fractions had the same mineral composition. For OK ore microwave treated for 8 and 15 min, the three size fractions were very similar with the exception

that the larger size fraction exhibited fewer olivine peaks than the two smaller size fractions. In contrast, XRD analysis of the untreated and microwave treated Pipe ore revealed that the mineral composition of the different size fractions varied, with magnetite, pyrrhotite and pentlandite concentrated in the smaller size fractions. In the Pipe ore treated with microwaves for 4 min, olivine was also concentrated in the two smaller size fractions while serpentine, quartz and cordierite were concentrated in the large size fraction (Figure 9). After 8 min of microwave treatment, the different size fractions of the Pipe ore exhibited more similar XRD patterns, although olivine, magnetite, pentlandite and pyrrhotite were still concentrated in the two smaller size fractions, and serpentine was concentrated in the >425 μm size fraction.

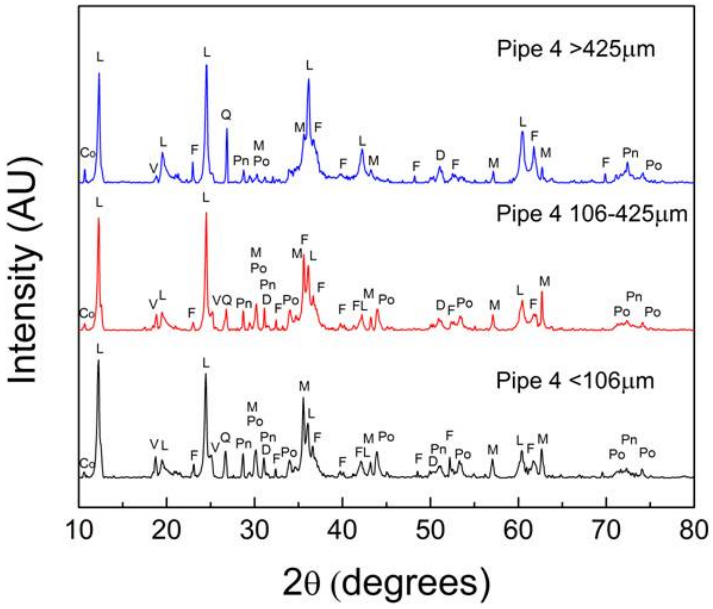

Figure 9. XRD patterns for Pipe ore microwave treated for 4 min, attrition milled for 15 min, and sieved into <106 μm, 106–425 μm, and >425 μm size fractions. Mineral phases identified include: cordierite (Co), dolomite (D), forsterite (F), lizardite (L), magnetite (M), pentlandite (Pn), pyrrhotite (Po), quartz (Q) and vermiculite (V).

The size-by-size XRD analysis of the OK and Pipe ores suggests that while minerals within the OK ore were evenly distributed and the ore texture was quite consistent, the opposite was true for the Pipe ore. In the OK ore, particles heated relatively evenly, and differences in particle heating were due primarily to the location of particles within the microwave reactor (particles near the centre of the microwave reactor heat better than samples near the reactor wall). The concentration of olivine in the smaller size fractions in the microwave treated OK ore indicates that particles that reached a higher temperature were more likely to break than other particles during grinding. In the Pipe ore, since the texture was inconsistent, some particles heated better in response to microwave radiation than others. Similar to the OK ore, particles that heated better also ground better in the Pipe ore, since olivine was concentrated in the smaller size fractions in the microwave treated Pipe ore. The fact that highly microwave responsive minerals, such as magnetite, pyrrhotite, and pentlandite, were also concentrated in the smaller size fractions suggests that particles that contained these minerals were heated preferentially and, therefore, ground preferentially. The textural differences between the OK and Pipe ore explains why the OK ore responded better to microwave assisted grinding than the Pipe ore, but does not explain why the grindability of the Pipe ore decreased with microwave pretreatment.

3.3.3. Hardness Measurements

Hardness measurement results for untreated and microwave treated OK and Pipe ores are shown in Figure 10. The results indicate that the hardness of both ores increased with increasing microwave

treatment. Since the primary reaction that occurs during microwave treatment is the conversion of serpentine to olivine, and olivine is reported to be harder than serpentine (Mohs hardness of 7 versus 2.5 [49]), this result is to be expected. While the increase in ore hardness with microwave treatment partially explains the decrease in grindability of the Pipe ore up to 4 min microwave treatment time, it does not explain the relative improvement in grindability after 8 min microwave pretreatment, and does not correlate with the improved grindability of the OK ore with increasing microwave treatment time.

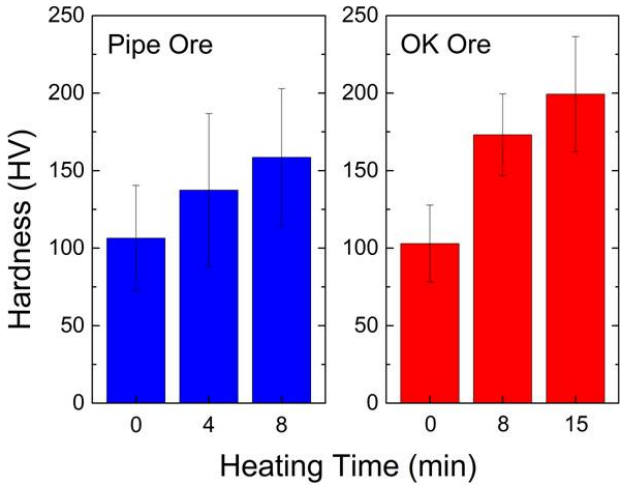

Figure 10. Micro-hardness results for untreated and microwave pretreated Pipe and OK ores [48].

3.3.4. Crack Analysis

During the examination of unground Pipe and OK ore particles by SEM, it was noted that significant cracking was present in microwave treated particles compared to the untreated particles. The cracking occurred along mineral grain boundaries, as well as in the bulk magnesium silicate (Figure 11). It is believed cracks formed along mineral grain boundaries due to thermal stresses generated by the differential heating of different minerals upon exposure to microwaves, and that the cracks formed in the bulk magnesium silicate due to the evolution of water vapor during serpentine dehydroxylation.

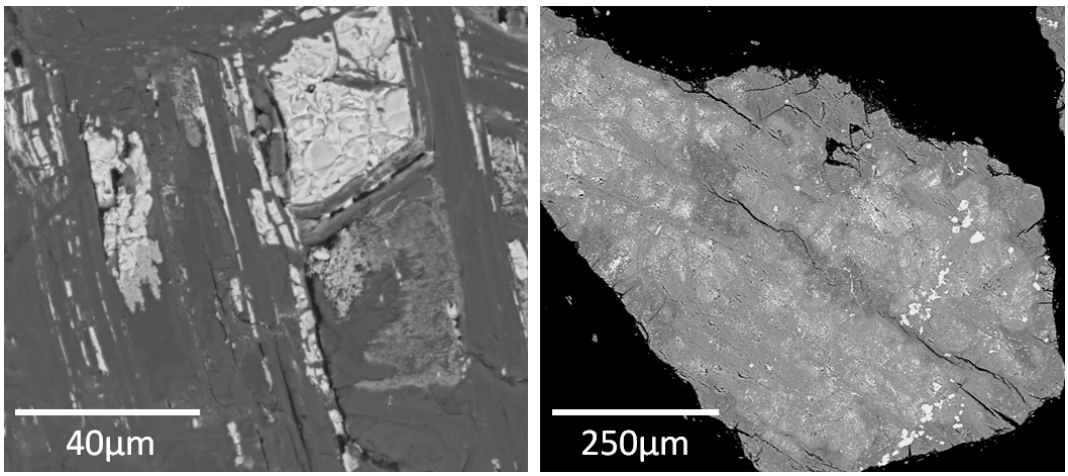

Figure 11. SEM-BSE images of particle cross-sections of crushed, unground (0.425–1 mm) OK ore microwave pretreated for 15 min. The image on the left depicts cracking along mineral grain boundaries, while the image on the right shows cracking in the bulk magnesium silicate [48].

The extent of cracking in untreated and microwave pretreated OK and Pipe ore was quantified, and the results are shown in Figure 12. The degree of cracking increased with increasing microwave treatment for both the OK and Pipe ores. For the OK ore, there was a substantial increase in crack length per unit area with each increment of microwave pretreatment. For the Pipe ore, there was a small average increase in crack length per unit area after 4 min microwave treatment; however, a substantial increase in cracking was not observed until after 8 min microwave pretreatment.

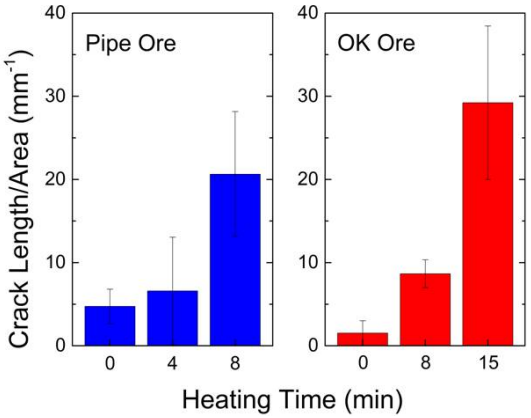

Figure 12. Crack length per unit area in untreated and microwave pretreated ores [48].

It appears that the OK ore grindability improved with increasing microwave pretreatment, despite increasing ore hardness, due to the cracking that occurred, both by the differential heating of different minerals and by the escape of water vapor due to serpentine dehydroxylation. Since highly microwave responsive minerals (such as iron oxides and sulphides) were well distributed within the OK ore, and since the OK ore had high serpentine content (84 wt %), cracking was systemic, and a great improvement in grindability was observed. For the Pipe ore, since highly microwave responsive minerals were not as well dispersed throughout the ore, cracking due to thermal stress was not as widespread. In addition, the Pipe ore contained less serpentine (63.7 wt %) than the OK ore and cracking due to the escape of water vapour during serpentine dehydroxylation was also less significant. Thus, as the Pipe ore became harder with increasing microwave treatment, the grindability of the ore decreased until sufficient cracking occurred to overcome the increase in hardness.

3.3.5. Pentlandite Liberation and Specific Surface Area

Pentlandite liberation for the Pipe and OK ores was found to increase with increasing microwave pretreatment time (Figure 13). The combination of microwave treatment and grinding was ultimately found to achieve greater pentlandite liberation at larger pentlandite P_{80} compared to samples that were ground for longer periods of time. Improved mineral liberation by microwave pretreatment has been reported by others. It is commonly understood that the mechanism of improved liberation as a result of microwave pretreatment is the differential heating of minerals within individual particles, leading to thermal stress and cracking along mineral grain boundaries [13,50]. Pentlandite liberation in the Pipe ore improved with increasing microwave treatment despite decreased grindability because cracking and particle breakage were concentrated in those particles that contained pentlandite.

The effect of microwave pretreatment on the specific surface area (SSA) of Pipe and OK ores is depicted in Figure 14. For up to 4 min heating time, the SSA of both ores was not affected. However, after 8 min microwave pretreatment, the SSA of both the Pipe and OK ore was greatly improved. At the maximum microwave pretreatment time (15 min for OK ore, 8 min for Pipe ore) the SSA of the OK and Pipe ores increased by an average of 3.2 and 1.7 times, respectively, for a given grinding time (15, 30 or 60 min). Similarly, the combination of maximum microwave pretreatment and grinding resulted in higher SSA for a given particle size compared to grinding alone.

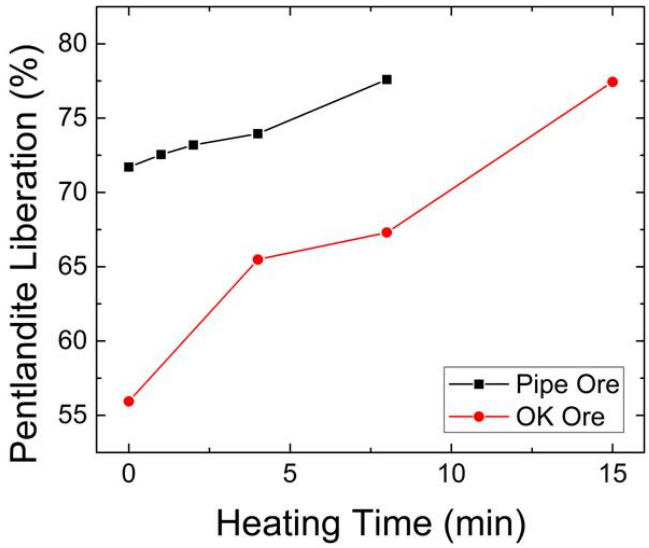

Figure 13. Pentlandite liberation versus microwave heating time after 15 min grinding for the Pipe and OK ores [48].

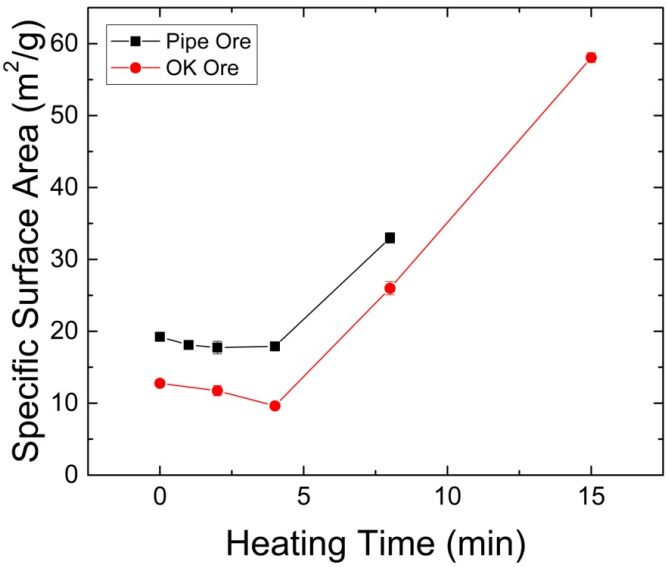

Figure 14. Specific surface area versus microwave heating time for Pipe and OK ores ground for 15 min [7].

The conversion of serpentine to olivine and resultant cracking is believed to be primarily responsible for the SSA trend with increasing microwave pretreatment for the Pipe and OK ores, as well as particle size. At microwave heating times of 4 min or less, cracking was due primarily to thermal stress between mineral grains of different composition. These cracks were small and contributed minimal surface area compared to the cracks generated by the release of water vapour during serpentine dehydroxylation at extended microwave heating times (8 min or more).

3.3.6. Energy Considerations

To determine if microwave pretreatment enhanced the efficiency of comminution for the two ultramafic nickel ores studied, the energy used in microwave treatment and grinding to achieve a certain product size was compared to that achieved with the energy used in grinding alone (Figure 15). It should be noted that the energy consumption of both microwave pretreatment (167 kWh/t per minute) and grinding (41 kWh/t per minute) was very high due to the small sample

sizes used and efforts have not been made to optimize energy usage at the lab scale. Overall, microwave treatment did not improve the energy used in grinding for the OK ore and increased the energy used in grinding for the Pipe ore. At first glance, this suggests microwave treatment is not a promising strategy to reduce the energy required for the processing of ultramafic ores. However, the improvement in pentlandite liberation suggests grinding need not be as fine to achieve mineral separation. Ultimately the energy used in microwave treatment needs to be weighed against overall process improvements, which may include improved grindability, as well as reduced slurry viscosity and yield stress [5] and enhanced flotation, dewatering and tailings treatment. Bobicki et al. [5] noted that if ultramafic nickel ore flotation pulp density could be increased from 20 to 30 wt %, as a consequence of improved slurry rheology attained by microwave pretreatment, the pulp volume and water usage could be reduced by 40%, likely resulting in significant savings in infrastructure and materials handling costs. Future work will further investigate the effects of microwave treatment on mineral liberation and energy usage in the processing of ultramafic ores, and will take into account effects on flotation, dewatering and tailings treatment.

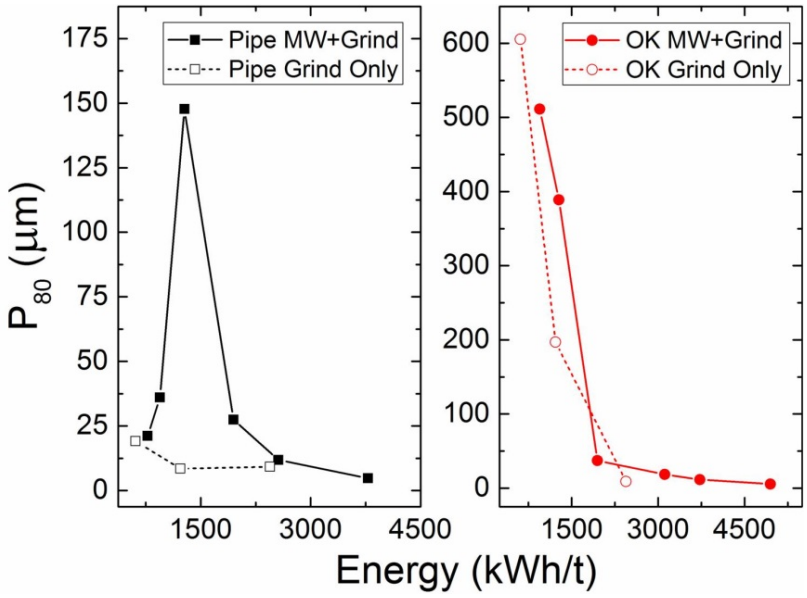

Figure 15. Sample P_{80} versus energy expended for Pipe and OK ore microwave pretreated and ground for various times (MW + Grind), or ground only for various lengths of time (Grind Only) [48].

4. Conclusions

Ultramafic nickel ores were found to heat well upon exposure to microwave radiation. The Pipe ore heated better than the OK ore, and the difference was attributed to the Pipe ore having higher imaginary permittitivies. The temperatures achieved during the microwave pretreatment of ultramafic nickel ores were sufficient to dehydroxylate serpentine; however, serpentine dehydroxylation was incomplete (serpentine content reduced from 84.0 wt % to 15.8 wt % for the OK ore and from 63.7 wt % to 23.7 wt % for the Pipe ore). FTIR analysis revealed that during serpentine dehydroxylation by microwave pretreatment, the serpentine brucite layer broke down prior to the siloxane layer. In addition to the dehydroxylation of serpentine, microwave treatment was found to convert pentlandite into another nickel phase that was not detectable by XRD. It was concluded from SEM-EDX analysis that the nickel remained in high-temperature phases after microwave pretreatment due to the slow kinetics of pentlandite/pyrrhotite exsolution under natural cooling conditions. The transition of pentlandite to other nickel phases as a result of microwave pretreatment may have implications for the upgrading of ultramafic nickel ores by flotation.

The grindability of the OK ore improved with increasing microwave pretreatment; however, the grindability of the Pipe ore decreased with moderate microwave pretreatment, and resembled that of the untreated ore after extended treatment. Increasing microwave pretreatment improved pentlandite liberation in both ores, and microwave pretreatment of 8 min or longer greatly improved the specific surface area of ground ores. It is believed that the grindability of the OK ore improved with increasing microwave pretreatment, despite increasing ore hardness, due to cracking generated in ore particles by the differential heating of different minerals and the release of water vapour due to serpentine dehydroxylation. Since the OK ore had a consistent texture, particles heated evenly in response to microwave radiation and cracking was widespread, leading to a great improvement in grindability. The texture of the Pipe ore was inconsistent and, thus some particles heated better than others and cracking was not as extensive as in the OK ore. As the Pipe ore became harder with increasing microwave pretreatment, the grindability of the ore decreased until sufficient cracking occurred to overcome the increase in hardness. Pentlandite liberation improved for both ores with increasing microwave pretreatment because cracking was concentrated in particles that contained microwave responsive minerals, such as pentlandite, pyrrhotite and magnetite. The improvement in specific surface area of the ores at longer microwave pretreatment times was linked to the conversion of olivine to serpentine: cracks due to the release of water from serpentine dehydroxylation were much larger, and contributed more surface area, than cracks that occurred due to thermal stress at lesser microwave pretreatment.

Ultimately, microwave pretreatment was not found to decrease the energy required for grinding ultramafic nickels ores under the conditions studied. However, the observed improvement in pentlandite liberation and specific surface area with microwave pretreatment suggests grinding need not be as fine for the upgrading of these ores. Future work will further explore the effects of microwave treatment on mineral liberation and energy usage in the processing of ultramafic ores, and will consider effects on rheology, flotation, dewatering, and tailings treatment.

Author Contributions: E.R.B. conceived, designed, and the conducted the experiments, analyzed the data and wrote the paper. Q.L. and Z.X. contributed reagents, materials, and analysis tools, and provided lab space, supervision and proofreading.

Funding: This research was funded by Vale Ltd. and a Collaborative Research and Development (CRD) Grant from NSERC (Natural Sciences and Engineering Research Council of Canada) entitled "An integrated strategy for CO_2 management and value creation form mine wastes", grant number CRDPJ 412287–2010.

Acknowledgments: This research was supported by Vale and a Collaborative Research and Development (CRD) Grant from NSERC (Natural Sciences and Engineering Research Council of Canada). The authors would also like to acknowledge Shiraz Merali, Gayle Hatchard, Jim Skwarok, Nancy Manchak, Joshua Neumann, Erin Furnell, John Forster, Manqiu Xu, and Andrew Lee for technical and laboratory assistance.

Conflicts of Interest: The authors declare no conflict of interest. The founding sponsors had no role in the design of the study; in the collection, analyses, or interpretation of data; in the writing of the manuscript, and in the decision to publish the results.

References

1. Yang, D.; Xi, L.; Bobicki, E.R.; Xu, Z.; Liu, Q.; Zeng, H. Probing anisotropic surface properties and interaction forces of chrysotile rods by atomic force microscopy and rheology. *Langmuir* **2014**, *30*, 10809–10817. [CrossRef] [PubMed]
2. Kusuma, A.M.; Liu, Q.; Zeng, H. Understanding interaction mechanisms between pentlandite and gangue minerals by zeta potential and surface force measurements. *Miner. Eng.* **2014**, *69*, 15–23. [CrossRef]
3. Xu, M.; Dai, Z.; Dong, J.; Ford, F.; Lee, A. Fibrous minerals in ultramafic nickel sulphide ores. In Proceedings of the 49th Conference of Metallurgists, Vancouver, BC, Canada, 3–6 October 2010; CIM: Westmount, QC, Canada, 2010; pp. 223–236.
4. Ndlovu, B.N.; Forbes, E.; Becker, M.; Deglon, D.A.; Franzidis, J.P.; Laskowski, J.S. The effects of chrysotile mineralogical properties on the rheology of chrysotile suspensions. *Miner. Eng.* **2011**, *24*, 1004–1009. [CrossRef]

5. Bobicki, E.R.; Liu, Q.; Xu, Z. Effect of microwave pre-treatment on ultramafic nickel ore slurry rheology. *Miner. Eng.* **2014**, *61*, 97–104. [CrossRef]
6. Senior, G.D.; Thomas, S.A. Development and implementation of a new flowsheet for the flotation of a low-grade nickel ore. *Int. J. Miner. Process.* **2005**, *78*, 49–61. [CrossRef]
7. Bobicki, E.R.; Liu, Q.; Xu, Z. Mineral carbon storage in pre-treated ultramafic nickel ores. *Miner. Eng.* **2014**, *70*, 43–54. [CrossRef]
8. Pickles, C. AMicrowaves in extractive metallurgy: Part 1—Review of Fundamentals. *Miner. Eng.* **2009**, *22*, 1102–1111. [CrossRef]
9. Haque, K.E. Microwave energy for mineral treatment processes—A review. *Int. J. Miner. Process.* **1999**, *57*, 1–24. [CrossRef]
10. Pickles, C.A. Microwaves in extractive metallurgy: Part 2—A review of applications. *Miner. Eng.* **2009**, *22*, 1112–1118. [CrossRef]
11. Radziszewski, P. Energy recovery potential in comminution processes. *Miner. Eng.* **2013**, *46–47*, 83–88. [CrossRef]
12. Amankwah, R.K.; Ofori-Sarpong, G. Microwave heating of gold ores for enhanced grindability and cyanide amenability. *Miner. Eng.* **2011**, *24*, 541–544. [CrossRef]
13. Kingman, S.W.; Jackson, K.; Cumbane, A.; Bradshaw, S.M.; Rowson, N.A.; Greenwood, R. Recent developments in microwave-assisted comminution. *Int. J. Miner. Process.* **2004**, *74*, 71–83. [CrossRef]
14. Walkiewicz, J.W.; Clark, A.E.; McGill, S.L. Microwave-assisted grinding. *IEEE Trans. Ind. Appl.* **1991**, *27*, 239–243. [CrossRef]
15. Henda, R.; Hermas, A.; Gedye, R.; Islam, M.R. Microwave enhanced recovery of nickel-copper ore: Comminution and flotability aspects. *Int. Microw. Power Inst.* **2005**, *40*, 7–16. [CrossRef]
16. Buttress, A.J.; Katrib, J.; Jones, D.A.; Batchelor, A.R.; Craig, D.A.; Royal, T.A.; Dodds, C.; Kingman, S.W. Towards large scale microwave treatment of ores: Part 1—Basis of design, construction and commissioning. *Miner. Eng.* **2017**, *109*, 169–183. [CrossRef]
17. Zhong, C.; Xu, C.; Lyu, R.; Zhang, Z.; Wu, X.; Chi, R. Enhancing mineral liberation of a Canadian rare earth ore with microwave pretreatment. *J. Rare Earths* **2018**, *36*, 215–224. [CrossRef]
18. Kingman, S.W.; Vorster, W.; Rowson, N.A. The influence of mineralogy on microwave assisted grinding. *Miner. Eng.* **2000**, *13*, 313–327. [CrossRef]
19. Forster, J.; Maham, Y.; Bobicki, E.R. Microwave heating of magnesium silicate minerals. *Powder Technol.* **2018**, *339*, 1–7. [CrossRef]
20. Liu, C.; Xu, Y.; Hua, Y. Application of microwave radiation to extractive metallurgy. *Chin. J. Metall. Sci. Technol.* **1990**, *6*, 121–124.
21. Dlugogorski, B.Z.; Balucan, R.D. Dehydroxylation of serpentine minerals: Implications for mineral carbonation. *Renew. Sustain. Energy Rev.* **2014**, *31*, 353–367. [CrossRef]
22. Berry, T.F.; Bruce, R.W. A simple method of determining the grindability or ores. *Can. Min. J.* **1966**, *7*, 63–65.
23. Hutcheon, R.M.; De Jong, M.S.; Adams, F.P. A system for rapid measurement of RF and microwave properties up to 1400 °C. *J. Microw. Power Electromagn. Energy* **1992**, *27*, 87–92. [CrossRef]
24. Robie, R.A.; Hemingway, B.S. *Thermodynamic Properties of Minerals and Related Substances at 298.15K and 1 Bar Pressure and at Higher Temperatures*; US Government Printing Office: Washington, DC, USA, 1995; Volume 2131, p. 470.
25. Bobicki, E.R.; Liu, Q.; Xu, Z. Microwave heating of ultramafic nickel ores and mineralogical effects. *Miner. Eng.* **2014**, *58*, 22–25. [CrossRef]
26. Fuchs, Y.; Linares, J.; Mellini, M. Mössbauer and infrared spectrometry of lizardite-1T from Monte Fico, Elba. *Phys. Chem. Miner.* **1998**, *26*, 111–115. [CrossRef]
27. Foresti, E.; Fornero, E.; Lesci, I.G.; Rinaudo, C.; Zuccheri, T.; Roveri, N. Asbestos health hazrd: A spectroscopic study of synthetic geoinspried F-doped chrysotile. *J. Hazard. Mater.* **2009**, *167*, 1070–1079. [CrossRef] [PubMed]
28. Mellini, M.; Fuchs, Y.; Viti, C.; Lemaire, C.; Linarés, J. Insights into the antigorite structure from Mössbauer and FTIR spectroscopy. *Eur. J. Miner.* **2002**, *14*, 97–104. [CrossRef]
29. Anbalagan, G.; Sivakumar, G.; Prabakaran, A.R.; Gunasekaran, S. Spectroscopic characterization of natural chrysotile. *Vib. Spectrosc.* **2010**, *52*, 122–127. [CrossRef]
30. Liu, K.; Chen, Q.; Hu, H.; Yin, Z. Characterization of lizardite in Yuanjiang laterite ore. *Appl. Clay Sci.* **2010**, *47*, 311–316. [CrossRef]

31. Fialips, C.; Petit, S.; Decarreau, A.; Beaufort, D. Influence of synthesis pH on kaolinite "crystallinity" and surface properties. *Clays Clay Miner.* **2000**, *48*, 173–184. [CrossRef]
32. Scholtzová, E.; Tunega, D.; Nagy, L.T. Theoretical study of cation substitution in trioctahedral sheet of phyllosilicates. An effect on inner OH group. *J. Mol. Struct. (Theochem)* **2003**, *620*, 1–8. [CrossRef]
33. Franco, F.; Pérez-Maqueda, L.A.; Ramírez-Valle, V.; Pérez-Rodríguez, J.L. Spectroscopic study of the dehydroxylation process of a sonicated antigorite. *Eur. J. Mineral.* **2006**, *18*, 257–264. [CrossRef]
34. Russell, S.D.J.; Longstaffe, F.J.; King, P.L.; Larson, T.E. The oxygen-isotope composition of chondrules and isolated forsterite and olivine grains from the Tagish Lake carbonaceous chondrite. *Geochem. Cosmochim. Acta* **2010**, *74*, 2484–2499. [CrossRef]
35. Makreski, P.; Jovanovski, G.; Stojančeska, S. Minerals from Macedonia XIII: Vibration spectra of some commonly appearing nesosilicate minerals. *J. Mol. Struct.* **2005**, *744–547*, 79–92. [CrossRef]
36. Frost, R.L.; Palmer, S.J.; Reddy, B.J. Near-infrared and mid-IR spectroscopy of selected humite minerals. *Vib. Spectrosc.* **2007**, *44*, 154–161. [CrossRef]
37. Alstadt, K.N.; Katti, D.R.; Katti, K.S. An in situ FTIR step-scan photoacoustic investigation of kerogen and minerals in oil shale. *Spectrochim. Acta Part A Mol. Biomol. Spectrosc.* **2012**, *89*, 105–113. [CrossRef] [PubMed]
38. Farmer, V.C. *The Infrared Spectra of Minerals*; Mineralogical Society: London, UK, 1974; p. 539.
39. Berry, A.J.; Hermann, J.; O'Neill, H.S.C.; Foran, G.J. Fingerprinting the water site in mantle olivine. *Geology* **2005**, *33*, 869–872. [CrossRef]
40. Trittschack, R.; Grobety, B. Dehydroxylation kinetics of lizardite. *Eur. J. Mineral.* **2012**, *24*, 47–57. [CrossRef]
41. Etschmann, B.; Pring, A.; Putnis, A.; Grguric, B.A.; Studer, A. A kinetic study of the exsolution of pentlandite $(Ni,Fe)_9S_8$ from the monosulfide solid solution (Fe,Ni)S. *Am. Mineral.* **2004**, *89*, 39–50. [CrossRef]
42. Wang, H. Isothermal kinetics of the pentlandite exsolution from mss/pyrrhotite using model-free method. *Tsinghua Sci. Technol.* **2006**, *11*, 368–373. [CrossRef]
43. Kullerud, G. Thermal stability of pentlandite. *Can. Mineral.* **1963**, *7*, 353–366.
44. Raghavan, V. Fe-Ni-S (Iron-Nickel-Sulfur). *J. Phase Equilibria Diffus.* **2004**, *25*, 373–381. [CrossRef]
45. Sugaki, A.; Kitakaze, A. High form pentlandite and its thermal stability. *Am. Mineral.* **1998**, *83*, 133–140. [CrossRef]
46. Kitakaze, A.; Sugaki, A.; Itoh, H.; Komatsu, R. A revision of phase relations in the system Fe-Ni-S from 650 °C to 450 °C. *Can. Mineral.* **2011**, *49*, 1687–1710. [CrossRef]
47. Kaya, E. Comminution behaviour of microwave heated two sulphide copper ores. *Indian J. Chem. Technol.* **2010**, *17*, 455–461.
48. Bobicki, E.R.; Liu, Q.; Xu, Z.; Manchak, N.; Xu, M. Effect of microwave pre-treatment on grindability of ultramafic nickel ores. In Proceedings of the 2013 Materials Science and Technology (MS&T), Montreal, QC, Canada, 27–31 October 2013.
49. RRUFF. Handbook of Mineralogy (PDF). 2012. Available online: http://rruff.geo.arizona.edu/doclib/hom/ (accessed on 9 January 2018).
50. Jones, D.A.; Kingman, S.W.; Whittles, D.N.; Lowndes, I.S. Understanding microwave assisted breakage. *Miner. Eng.* **2005**, *18*, 659–669. [CrossRef]